

Egyptian Journal of Chemistry

http://ejchem.journals.ekb.eg/



Silver Nanoparticles as Fuel Additives: Influence on Gasoline Octane Number and Flash Point



¹Petrochemical Engineering Department , Faculty of Engineering, MiniaUniversity, Egypt.

²Chemical Engineering Department, Faculty of Engineering, Minia University, Egypt.



Abstract

In this work an alternative of improving the quality of gasoline by the use of silver nanoparticles (AgNPs) as fuel additives is proposed, measured by two important parameters include octane number and flash point. The synthesis of AgNPs was done by a green technique and the solution was added into gasoline in different concentrations (0.1-5.0 g L⁻¹), where the treated samples of the fuel were also subject to standard ASTM testing procedures. The findings showed that there was a significant change in octane number. The results revealed a notable increase in octane number from 80 % to 87 %. This was due to catalytic characteristics of AgNPs that promote efficiency in the combustion. At the same time, the flash point improved from -43° C to -39.5 °C, being a sign of increased thermal stability and safer handling properties of fuels. The overall results of statistical analysis in a quadratic model supported the known fact that the concentration of nanoparticle was the greatest impact on both responses, whereas time and temperature had minor influence. The model was also valid as shown using diagnostic plots ($R^2 = 0.986$ for octane number, $R^2 = 0.963$ for flash point). This is evidenced by the results that the AgNPs has great potential of enhancing the fuel properties at low dose thus being scalable and environmentally friendly. This novel study highlights the growing presence of nanotechnology in the fuel engineering field, and shows one avenue towards future studies in the use of nanoparticle combustion enhancement methods.

Keywords: Nanomaterials, Gasoline, Octane Number, Flash Point

1. Introduction

The modern-day gasoline engines require the use of high-performance fuel capable of carrying out efficient combustion with a minimal effect on the environment. Knocking, incomplete burning and dangers caused by volatility are some of the limitations that traditional formulations of fuel are firmly faced with. Researchers have in their turn shifted their attention to the addition of nanomaterials to improve the quality and performance of gasoline [1]. Nanomaterials have potentials of enhancing fuel properties, in terms of octane number, flash point, engine performance, and emissions pattern due to the high surface area, catalytic activity, and modification possibilities [2-5].

To improve the deficiency in octane value of gasoline, the octane number should be improved, making gasoline less prone to knocking, which improves smooth engine run as well as increased life of the engine. The flash point can be adjusted so that it can affect safety of fuel during storage and handling. More to the point, the maximization of these properties would also lead to improved combustion efficiency, lower fuel consumption, and lower emissions, which are the primary objectives of both the energy and environmental policies. This research paper presents a new amalgamation of silver nanoparticles (AgNPs) with a view of investigating their impacts on the physicochemical as well as performance-inducing qualities of gasoline.

Past research has established that: Nanotechnology has transformed the oil and gas industry such that all processes are affected including upstream, exploration, downstream process, and environmental restoration

*Corresponding author e-mail: aya.mohsen@mu.edu.eg

Received Date: 20 June 2025, Revised Date: 06 July 2025, Accepted Date: 16 August 2025

DOI: 10.21608/EJCHEM.2025.396080.11929

processes [6]. Several types of nanomaterials, including metal oxides (Titanium dioxide (TiO₂), Aluminum oxide (Al₂O₃)), carbon nanotubes (CNTs), and silver-composed composite have been adapted to their catalytics and adsorption potentials to enhance fuel quality and environmental performance [7-10].

Particularly, functionalized carbon nanotubes CNTs and especially those modified with amide groups have proved to have a significant capacity in raising the octane number of gasoline [1]. In the same way, oxygen carrier nanomaterials (e.g. ethanol- mixed metal oxides) enhance combustion by increasing the oxygen concentration of the fuel, resulting in enhanced performance and reduced emission levels [1, 7, 11]. Such metal oxides as TiO₂ and Al₂O₃ are effective catalysts, nanolubricants, fuel efficiency as well as engine operation [1]. Overall general research has revealed that using nano sized fuel additives has the advantages of enhancing the combustion catalytic efficiency, complete fuel combustion, and is beneficial in the engine performance [8, 12, 13].

Despite these advancements, there is limited direct research on the impact of specific nanomaterials particularly bentonite and silver on gasoline's flash point and fuel behavior, which necessitates further investigation [1]. However, silver and silver-based nanocomposites synthesized using the pulsed laser ablation in liquid (PLAL) method have shown strong crystallinity and plasmonic behavior, making them promising for petroleum detection and sensor applications [9].

Fuel additives such as ethanol, methyl tert-butyl ether (MTBE), and prenol have long been recognized for their role in improving combustion efficiency and suppressing engine knocking in spark-ignition engines[14]. These components adjust volatility and increase octane numbers, thereby enhancing engine performance and reducing harmful emissions [12, 15, 16]. Studies involving a wide range of additives including bioethanol, MTBE, 2-methyl-1-propanol, Zinc oxide (ZnO), Zirconium dioxide (ZrO₂), and CNTs demonstrated significant improvements in fuel characteristics. Notably, these additives boosted octane numbers, engine torque, and power output while reducing Carbon monoxide (CO), Carbon dioxide (CO₂), and unburned hydrocarbons by up to 80% [7]. Fuzzy modeling approaches confirmed that blending renewable additives into hydrocracked gasoline can yield higher-octane, cleaner fuels[16].

Advanced octane enhancers like bioethanol, prenol, furan mixtures, dimate, and isooctene also exhibit synergistic effects, providing both performance and environmental benefits when added to low-octane hydrocarbon streams [17]. These compounds are gaining attention as practical solutions to meet global demands for high-efficiency, eco-friendly fuels.

Bentonite clay, known for its high surface area and cation exchange capacity, can be modified using agents such as cetyltrimethylammonium bromide (CTAB) to produce nano-bentonite with improved properties. This enhanced material is widely used in catalysis, water treatment, and drilling applications [18]. For instance, bentonite-derived nano-silica catalysts supported with HY-zeolite have shown high efficiency in the oxidative desulfurization of kerosene, achieving sulfur removal rates of up to 87.88%. Further process optimization has allowed for sulfur elimination exceeding 99%, as confirmed by modeling and characterization techniques [19].

In the realm of environmental remediation, petroleum hydrocarbon pollution remains a serious concern due to its toxicity and persistence. Traditional physicochemical methods often fall short, whereas nano-bioremediation leveraging the interaction of nanoparticles with microbes and enzymes offers a more sustainable, cost-effective, and efficient approach. This strategy enhances microbial activity and pollutant degradation, while also enabling enzyme immobilization through nano-supports, pointing to a strong future potential in environmental cleanup efforts[20].

The selection of Ag/AgCl nanoparticles in this study was primarily based on their catalytic activity, cost considerations, and environmental impact, particularly when synthesized using Jatropha plant extract. First, regarding catalytic activity, Ag/AgCl nanoparticles possess strong oxidative and catalytic properties that promote enhanced combustion efficiency and more complete fuel oxidation, leading to improved energy release and reduced harmful emissions. When synthesized using Jatropha extract, additional bioactive surface functionalities further support these catalytic effects. Second, in terms of cost, although silver is typically more expensive, the use of green synthesis with Jatropha significantly reduces overall processing costs by eliminating the need for

hazardous chemicals and high-energy equipment. Moreover, only minimal nanoparticle dosages are required to achieve noticeable performance improvements, making the approach economically viable. Finally, from an environmental perspective, the green synthesis route using Jatropha extract offers a sustainable and eco-friendly alternative to conventional chemical or physical synthesis methods. Jatropha is a non-edible, widely available plant that enables the production of biogenic nanoparticles with minimal ecological footprint, avoiding secondary pollution and reducing the risk of toxic residues. Therefore, the combination of high catalytic efficiency, manageable cost, and favorable environmental profile strongly supports the choice of Jatropha-based Ag/AgCl nanoparticles as promising fuel additives.

Recent catalytic innovations such as the development of silver dichromate-geopolymer composites have introduced new pathways for simultaneous desulfurization and denitrogenation. These materials present a promising solution for cleaner fuel production, aligning with global sustainability goals [12, 21, 22]. Collectively, these studies underscore the versatile and growing role of nanomaterials and additives in modern petroleum science. From enhancing fuel performance and emissions reduction to environmental remediation and sensor development, nanotechnology continues to shape the future of the energy sector.

Despite promising findings, there is still a knowledge gap regarding how non-carbon-based nanomaterials, such as silver nanoparticles impacts both octane number and flash point in gasoline[23-25]. Most existing research focuses on diesel or biofuels, with limited data on gasoline-specific applications[26-29]. Therefore, the primary objective of this study is to evaluate the influence of these nanomaterials on the octane rating, flash point, and overall combustion behavior of gasoline. The research aims to provide a scientific basis for developing enhanced, safer, and more environmentally friendly fuel formulations using nanoscale additives.

2. Methodology

This experimental study was conducted to investigate the effects of silver nanoparticles (AgNPs) on the physicochemical properties of gasoline with an 80 octane rating and flash point $-43\,^{\circ}\text{C}$. The nanoparticles were locally synthesized using green and mechanical methods to ensure cost-effectiveness and environmental sustainability. Silver nanoparticles were prepared through a biological reduction process using plant extract.

2.1. Fuel Preparation

Commercially available 80 octane gasoline was used as the base fuel. The nanoparticles were added to the fuel at a concentration of (0.1 g to 5 g) L⁻¹ of gasoline. The experimental apparatus was a vertical reactor tower having six stages, which was custom made. A total fuel volume of 1L was introduced from the top and distributed evenly across all stages to maximize the contact surface area between the nanoparticles and the gasoline, thereby promoting better interaction and achieving a more homogeneous mixture. The residence time was set according to the experimental matrix (ranging from 1 to 10 hours). The system was operated under controlled temperatures between 15 °C and 45 °C. This design allowed precise adjustment of contact time and temperature to optimize nanoparticle dispersion and ensure complete homogenization . The intentional distribution of nanoparticle concentration in each stage was aimed at achieving uniform dispersion within the fuel and ensuring consistent interaction between the nanoparticles and fuel components. Additionally, continuous mechanical stirring at 500 rpm was applied for 15 minutes at the beginning of the reaction to further promote initial dispersion and enhance contact between the nanoparticles and the fuel. In all 17 fuel samples were prepared to methodically explore the impact of the nanoparticle on the characteristics of gasoline. In order to obtain statistical reliability as well as the optimization of the used conditions, Design expert software (version 12) was used to determine the experimental matrix and analyze results. In this way, it was possible to assess the main effects and the interactions between the variables efficiently so that a more precise idea of the effect of nano-additives on the performance and safety parameters of the fuel could be formed. The matrix of the experimental design is found in Table 1. All experiments were designed using Design Expert software, which included replicated runs to assess experimental error and ensure statistical validity. In addition, all key measurements were performed in duplicate (n = 2) to further enhance data reliability and confirm reproducibility.

Table1: Experimental design matrix.

Std (Standard order)	Run	Time (hr)	Temperature (°C)	Concentration (g)
1	1	1	15	2.55
17	2	5.5	30	2.55
14	3	5.5	30	2.55
16	4	5.5	30	2.55
11	5	5.5	15	5
15	6	5.5	30	2.55
4	7	10	45	2.55
7	8	1	30	5
5	9	1	30	0.1
10	10	5.5	45	0.1
12	11	5.5	45	5
6	12	10	30	0.1
9	13	5.5	15	0.1
3	14	1	45	2.55
2	15	10	15	2.55
13	16	5.5	30	2.55
8	17	10	30	5

2.2. Nanomaterials Preparation

2.2.1. Materials

Silver nitrate (AgNO₃, 99.9 purity) was bought at Al-Safa chemicals Company, at Minya, Egypt. Jatropha seeds were sourced in local farms around Luxor, Egypt. Aqueous plant extract was prepared by thoroughly washing and boiling the seeds in distilled water as a natural reducing and stabilizing agent in the green synthesis of silver nanoparticle.

2.2.2. Preparation of Silver Nanoparticles (AgNPs)

Silver nanoparticles were synthesized using a green synthesis approach[30-32]. Aqueous extract of Jatropha Plant was used as a natural reducing and stabilizing agent[33-37]. During a typical procedure, a 50 mL solution of 1 mM of silver nitrate (AgNO₃) reagent was added to 10 mL of the plant extract with constant stirring at room temperatures. The AgNPs were formed as the reaction mixture turned to yellow and finally to dark brown color. 24 hours were given to the solution to settle after which they would be centrifuged at 10, 000 rpm within 15 minutes. The resultant pellet was subsequently washed thrice using deionized water and then dried at a temperature of 60 °C in order to obtain powdered silver nanoparticles.

2.3. Characterization and Testing:

The right characterization methods were used to analyze the structural and morphological properties of the synthesized nanomaterials, Transmission Electron Microscopy (TEM) was used to study the shape, dispersion, and approximate size of the nanoparticles on the nanoscale level since they were biosynthesized silver nanoparticles. Also, X-ray Diffraction (XRD) analysis was performed to check on the phase combination as well as the crystalline structure of Silver nanoparticles. These methods gave important data on the morphology and structural integrity of the synthesized nanomaterials which are essential in determining the performance of nanomaterials in fuels applications.

2.3.1. Experimental Determination of Octane Number

The octane rating of gasoline samples was determined by the use of Research Octane Number (RON) method; this method is widely being used in petroleum refineries and fuel quality laboratories.[38, 39]. The test was carried out concerning ASTM D2699 standard, and the test was done using a CFR (Cooperative Fuel Research) engine which is specially used to determine the octane rating of a fuel. Under constant temperature and pressure of this mode, the engine rotates at the fixed speed of 600 revolutions per minute (RPM). The RON indicates the ability of the fuel to resist knocking under fairly moderate operational regimes, eg low speed, city-driving operation. The comparison of the fuel of the test with a blend of iso-octane (high anti-knock) and n-heptane (low anti-knock) is recorded in the test. [40, 41]. The more resistance to knocking the fuel will have, the higher the value of RON will be. This was chosen in that it is relevant to a real-life situation on engine performance and it is commonly used in rating commercial gasoline grades. [42-44].

2.3.2. Experimental Determination of Flash Point

The flash point of the gasoline samples was determined using the Pensky-Martens closed cup method, following the ASTM D93 standard[41, 45-47]. The technique is common in the petroleum field where it helps to test the degree of volatility and flammability of liquid fuels. In close cup test a given quantity of the sample is put in a closed cup and slowly heated under a controlled rate. An ignition source is periodically entered, and the temperature of which a visible flash is observed is then recorded as the flash point. The closed cup method gives a more realistic representation of the field environment of storage and handling than does the open cup method since vapor loss is minimized and the effects of the external world reduced [48, 49]. The flash point is important in determining the safety of fuel when being stored, transported and used especially in the essentiality of fuels that have volatile compounds or compounds like nanomaterials which are added to the fuel.

3. Results and Discussion

3.1. XRD analysis

The synthesized nanomaterials require a detailed characterization in order to capture the physicochemical properties of the materials completely. Techniques of characterization include structural, morphological, and crystalline characteristics of nanomaterials that directly affect activity and possible uses of nanomaterials. This research involved the use of two important analytical methods which are X-ray diffraction (XRD) and Transmission Electron Microscopy (TEM) [50]. XRD allows one to determine the crystalline structure, the phase composition, and average crystallite size of nanomaterials, based on the analysis of their diffraction patterns [51]. It also allows determining phases like metallic silver (Ag), silver chloride (AgCl) and has data on crystallinity and purity [52]. Contrarily, TEM provides a high resolution image to determine the morphology, the size distribution of particles, shape and the internal structure of the nanoparticles at the nanodimensional level. It enables one to see directly the nature of the surface of the nanomaterial and its tendencies to agglomerate.

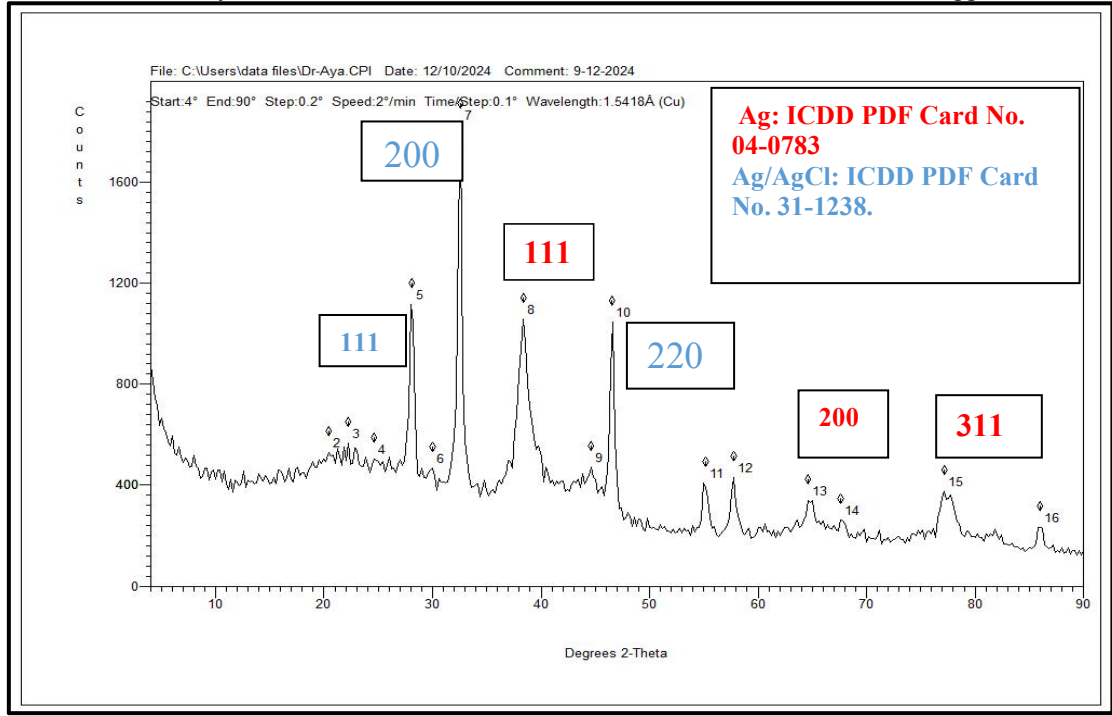


Figure 1: XRD pattern of silver nanoparticles synthesized using Jatropha seeds extract

The X-ray diffraction (XRD) analysis of the synthesized nanomaterials revealed distinct peaks at 20 values of approximately 27.8°, 32.2°, 38.1°, 44.3°, 46.3°, 64.4°, and 77.4°. These diffraction peaks were identified based on standard data from the International Centre for Diffraction Data (ICDD, formerly JCPDS). The peaks at 38.1°, 44.3°, 64.4°, and 77.4° were assigned to the (111), (200), (220), and (311) planes of face-centered cubic (FCC) silver (Ag), in agreement with ICDD PDF Card No. 04-0783. Meanwhile, the peaks at 27.8°, 32.2°, and 46.3° correspond to the (111), (200), and (220) planes of silver chloride (AgCl), matching ICDD PDF Card No. 31-1238.

The simultaneous presence of both Ag and AgCl phases indicates that silver ions (Ag⁺) were partially reduced to elemental silver and partially converted to AgCl due to the presence of chloride ions in the Jatropha plant extract. This supports the successful green synthesis of Ag/AgCl nanocomposites, where the extract acted both as a reducing agent and a natural chloride source. Similar outcomes have been reported in recent studies on green-mediated synthesis of silver-based nanoparticles using plant extracts containing inherent halides[53]. The average crystallite size (D) of the synthesized nanoparticles was estimated using the Scherrer equation (1) based on the broadening of the most intense diffraction peaks [54, 55]:

$$D = \frac{K.\lambda}{\beta.\cos\theta} \quad (1)$$

where D is the crystallite size (nm), K is the shape factor (typically 0.9), λ is the X-ray wavelength (1.5418 Å for Cu-K α), β is the full width at half maximum (FWHM) of the selected diffraction peak in radians, and θ is the Bragg angle (in radians). The FWHM values were corrected to remove instrumental broadening, and the calculations were performed for the main diffraction peaks corresponding to both Ag (metallic silver) and AgCl (silver chloride) phases. The resulting crystallite sizes were found to be in the range of 10-30 nm, indicating the nanocrystalline nature of the synthesized Ag/AgCl material. These results support the nanoscale size indicated by TEM, and confirm that the biosynthesis process using Jatropha extract effectively produced well-defined nanocrystalline particles. As shown in Figure 1 and Table 2 the XRD pattern confirms the presence of both Ag and AgCl phases.

Table 2: XRD Peak Positions and Phase Identification of Ag/AgCl Nanoparticles with Calculated Diameter (Scherrer Equation).

2θ (°)	Phase	Plane (hkl)	ICCD PDF No.	Diameter (nm)	Remarks
27.8	AgCl	(111)	31-1238	8.408	Crystalline silver chloride
32.2	AgCl	(200)	31-1238	27.615	
38.1	Ag	(111)	04-0783	2.823	Strong, characteristic of Ag FCC
44.3	Ag	(200)	04-0783	2.88	
46.3	AgCl	(220)	31-1238	11.613	Overlapping region
64.4	Ag	(220)	04-0783	4.698	
77.4	Ag	(311)	04-0783	2.1	High-angle silver reflection

3.2.TEM analysis:

Transmission Electron Microscopy (TEM) was conducted to investigate the morphology, size distribution, and structural arrangement of the synthesized Ag/AgCl nanocomposite. The TEM micrographs revealed a heterogeneous mixture of spherical to quasi-spherical nanoparticles with sizes typically ranging from 10 to 30 nm. The particles exhibited relatively uniform dispersion with some degree of agglomeration, which is commonly attributed to the presence of natural phytochemicals from the Jatropha extract acting as capping and stabilizing agents.

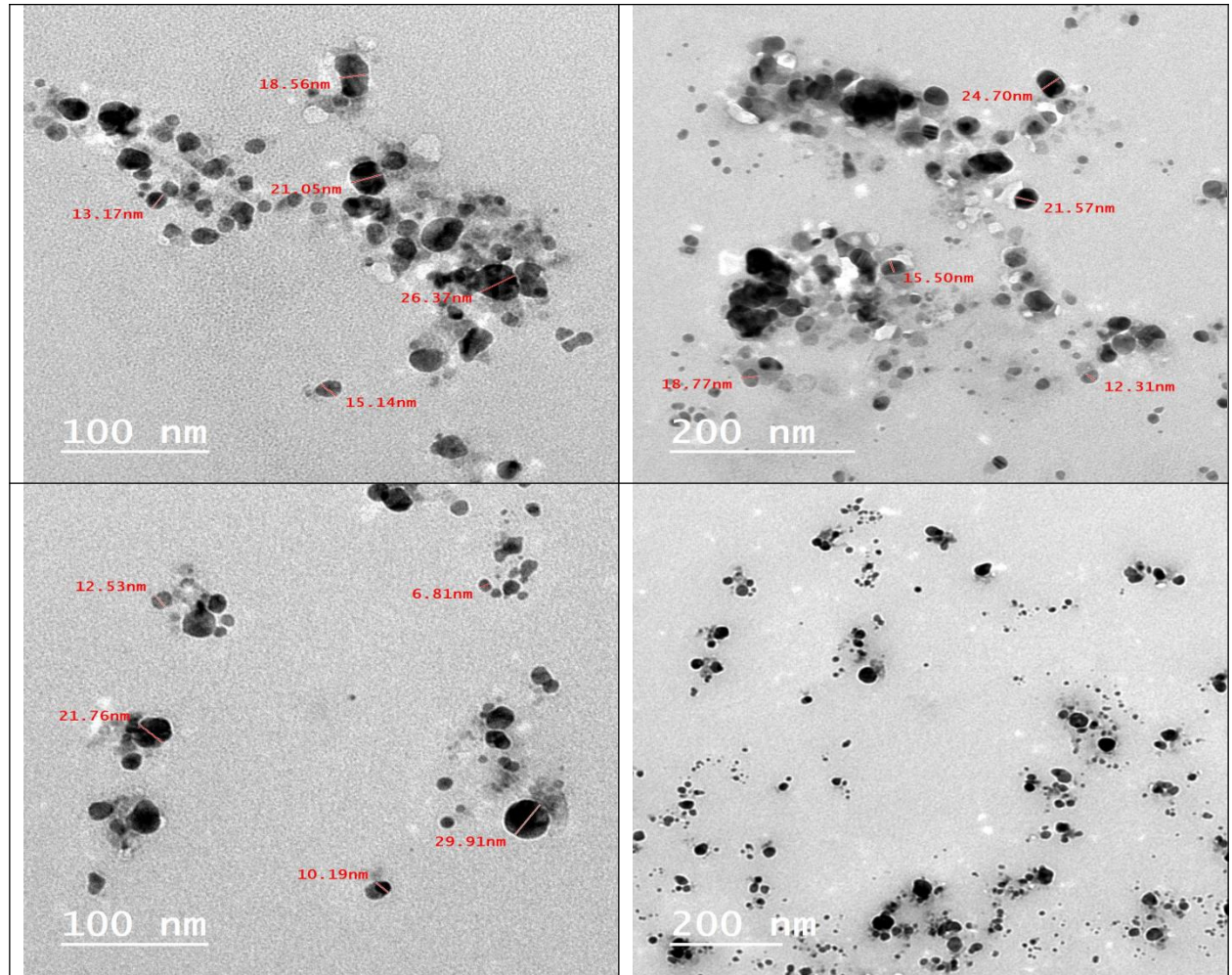


Figure 2. TEM micrograph of Ag/AgCl nanocomposite synthesized using Jatropha extract.

The contrast observed in the TEM images suggested the coexistence of two distinct phases within the nanocomposite. The darker regions are attributed to metallic silver nanoparticles (Ag⁺), which exhibit higher electron density due to their higher atomic number, while the lighter or less dense regions correspond to silver chloride (AgCl). This phase distinction is a typical feature of Ag/AgCl hybrid nanostructures synthesized via green routes. The formation of this composite structure confirms the dual role of Jatropha extract as both a reducing agent (for Ag⁺ to Ag⁰) and a chloride ion donor (facilitating AgCl formation). These observations are in strong agreement with the XRD results, which also confirmed the presence of both Ag and AgCl phases. Figure 2 illustrates uniform Ag /AgCl nanoparticles.

The nanoparticles exhibited an average diameter of $13.407 \text{ nm} \pm 7.3 \text{ nm}$ (mean \pm SD), indicating a relatively broad size distribution, which is commonly observed in green synthesis approaches due to the natural variability of bioactive reducing agents. This broad distribution reflects the inherent characteristics of plant-mediated synthesis methods, where multiple bioactive compounds simultaneously influence nucleation and growth processes. The particle size distribution of the synthesized nanoparticles is illustrated in Figure 3, confirming the relatively broad size distribution and supporting the TEM observations.

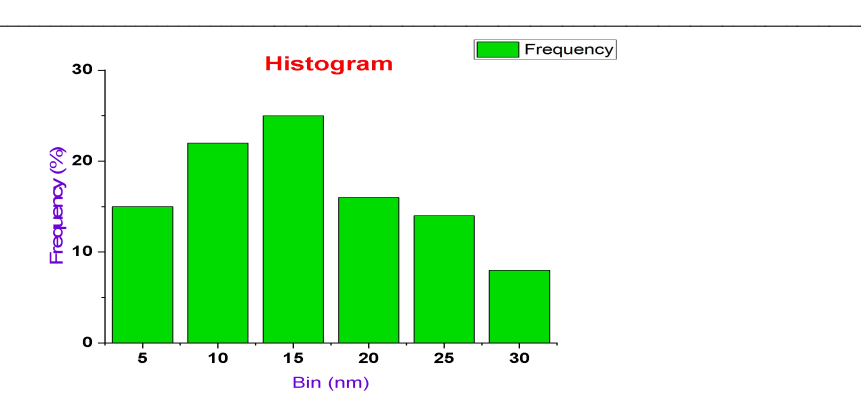


Figure 3. Particle size distribution histogram of biosynthesized Ag/AgCl nanoparticles derived from Jatropha extract, showing mean diameter of 13.4 nm \pm 7.3 nm.

3.2. Effect of Nanomaterials on Fuel Properties

3.2.1. Effect on Octane Number

In this study, the F-value (variance ratio) is used to evaluate the overall significance of the regression model, while the p-value indicates the probability level of each factor's effect. A smaller p-value suggests a more significant effect. The quadratic ANOVA model revealed a highly significant relationship between the independent variables and the octane number of gasoline enhanced with silver nanoparticles (AgNPs), as evidenced by the overall model significance (F = 1887.76, p < 0.0001). Among the main effects, the AgNPs concentration (C) had the most pronounced influence with an F-value of 16129.80, indicating a dominant role in enhancing octane rating. Temperature (B) and time (A) also showed statistically significant effects with F-values of 268.28 and 216.85, respectively (p < 0.0001 for both). The interaction effects revealed that AC (Time × Concentration) and BC (Temperature × Concentration) were significant (F = 90.24 and 14.44; F = 0.0001 and 0.0067, respectively), suggesting synergistic effects between these parameters. However, the AB interaction (Time × Temperature) was not significant (F = 0.3093), indicating no combined effect. The quadratic terms A² and C² were also significant (F = 0.005), reflecting non-linear behavior, while B² was not significant (F = 0.9136). The lack of fit test was not significant (F = 0.5689), confirming that the model fits the experimental data adequately without systematic error. Table 3 presents the ANOVA results, indicating which variables had a statistically significant effect on the octane number after the addition of AgNPs.

These findings strongly support the conclusion that AgNPs, especially at optimized concentrations and conditions, significantly enhance the octane number, making them a promising additive in fuel enhancement applications.

Source	p-value	F-value	Significance
A - Time	< 0.0001	216.85	Significant
B - Temperature	< 0.0001	268.28	Significant
C - Concentration	< 0.0001	16129.80	Highly significant
AB	0.3093	1.20	Not significant
AC	< 0.0001	90.24	Significant
BC	0.0067	14.44	Significant
A ²	0.0029	19.90	Significant
B ²	0.9136	0.0126	Not significant
C ²	< 0.0001	239.67	Highly significant
Lack of Fit	0.5689	0.7676	Not significant (Good
			fit)

Table 3: ANOVA table for octane number with AgNPs treatment

3.2.1.1. Final equation in terms of actual factors:

The octane number (ON) as a function of time (A), temperature (B), and AgNPs concentration (C) can be expressed by the following quadratic model equation (2):

Octane No = $79.45 + 0.0965 A + 0.0127 B + 1.4563 C - 0.00033 AB + 0.0295 AC + 0.0021 BC - 0.0073 A^2 - 0.000006 B^2 - 0.0860 C^2$ (2)

The quadratic regression model derived for the octane number clearly demonstrates the influence of time (A), temperature (B), and AgNP concentration (C), along with their interaction and squared effects. The positive coefficients of the linear terms for A, B, and especially C (1.4563) indicate that increasing these parameters tends to enhance the octane number, with the concentration of silver nanoparticles being the most impactful. Significant interaction terms (AC and BC) also suggest a synergistic behavior between parameters, while the negative coefficients of the quadratic terms (A² and C²) reflect a diminishing return effect at higher values. The derived model equation is essential in predicting and optimizing operating conditions for maximum octane improvement using AgNPs.

To assess the validity and reliability of the regression model used for predicting the octane number in response to silver nanoparticle (AgNP) treatment, several diagnostic plots were analyzed, as presented in Figure 4. The normal probability plot of residuals (Figure 4a) shows that the data points closely follow the diagonal line, indicating that the residuals are approximately normally distributed and that the assumption of normality is satisfied. Figure 4b, which plots residuals versus predicted values, reveals that the residuals are randomly scattered around zero, with no evident pattern or funnel shape. This randomness suggests homoscedasticity, meaning the variance of residuals is constant across all levels of prediction—a key assumption of ANOVA. In Figure 4c, Cook's distance plot indicates that none of the experimental runs have a disproportionately large influence on the model, as all points fall well below the threshold of concern (typically 1), confirming the robustness of the model. Finally, the Box-Cox plot (Figure 4d) shows that the confidence interval for the best lambda value includes 1, suggesting that no power transformation is required and the model is already in an optimal form for analysis. Collectively, these diagnostic plots validate the adequacy of the model and confirm that the data meet the assumptions necessary for reliable interpretation.

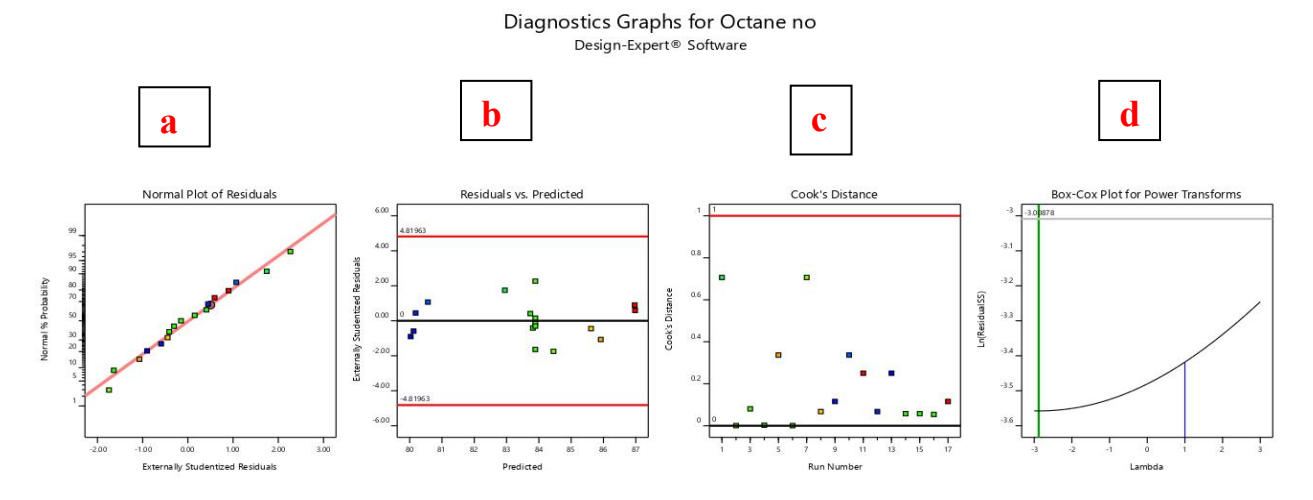


Figure 4: Diagnostic plots for the octane number model: (a) normal probability plot of residuals, (b) residuals versus predicted values, (c) Cook's distance plot for influential points, and (d) Box-Cox plot for assessing the need for data transformation.

The two-dimensional contour plots presented in Figure 5 illustrate the effects of silver nanoparticle (AgNP) concentration, reaction time, and temperature on the octane number of gasoline. In Figure 5a, the interaction between temperature and AgNP concentration at a constant time of 5.95 hours is shown. A noticeable gradient is observed, where the octane number increases steadily with both increasing temperature and nanoparticle concentration, highlighting a synergistic influence of thermal energy and particle availability. Figure 5b focuses on the influence of time and concentration at a constant temperature of 35 °C. The contour lines demonstrate that

longer reaction times combined with higher concentrations result in significant octane improvement, reaching values as high as 86%, which reinforces the catalytic effect of AgNPs over time. In Figure 5c, the interaction between time and temperature is examined at a constant concentration of 2.06 g L⁻¹. Here, the contour lines are nearly parallel and the range of octane number variation is narrow, suggesting a relatively weak combined effect of time and temperature at this low concentration level. Overall, these plots confirm that AgNP concentration is the most influential factor, while time and temperature have secondary but supportive roles in enhancing the octane number of gasoline.

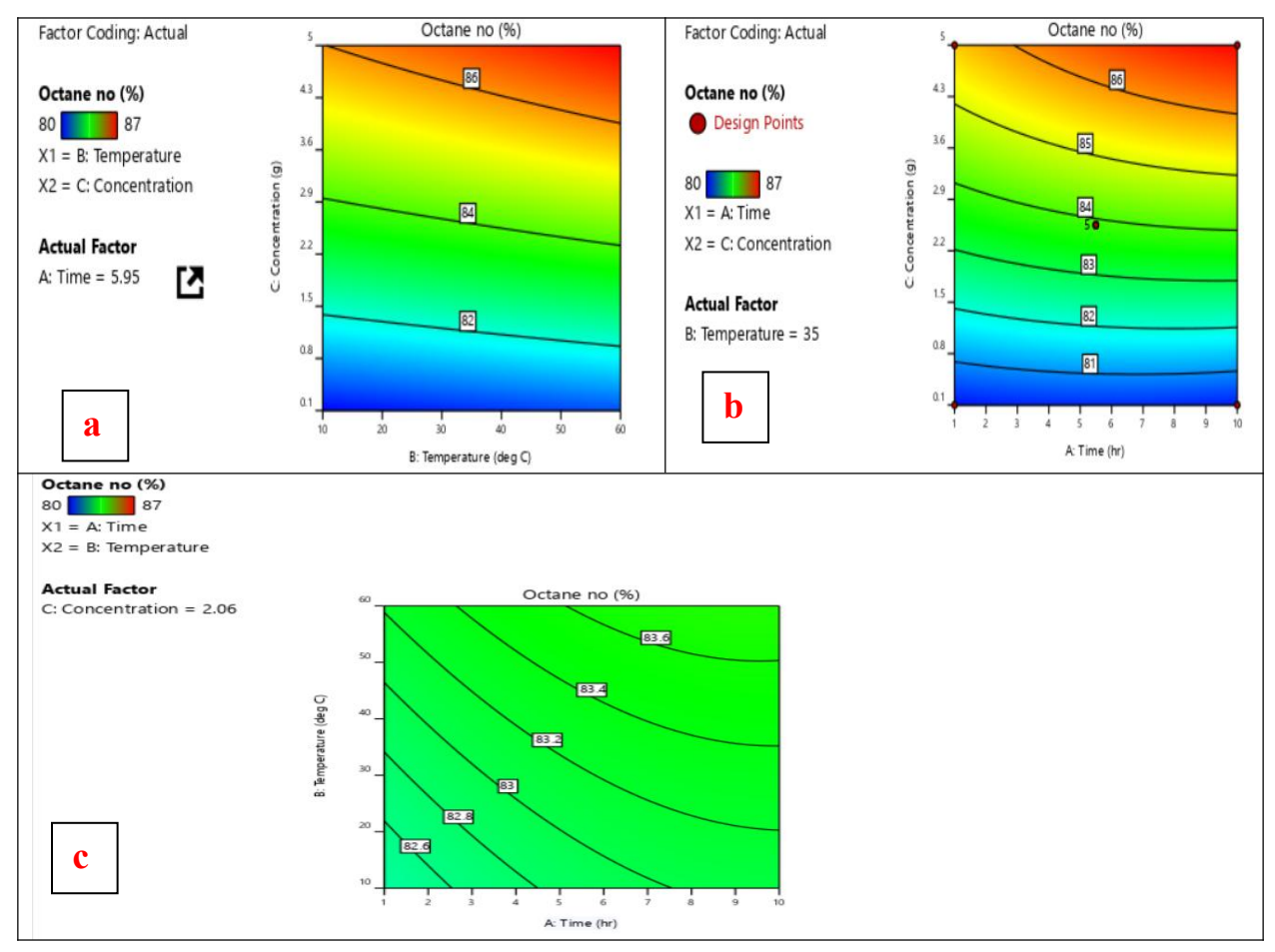


Figure 5: Two-dimensional contour plots showing the effect of silver nanoparticle concentration, temperature, and time on octane number: (a) concentration vs. temperature at fixed time, (b) concentration vs. time at fixed temperature, and (c) temperature vs. time at fixed concentration.

The effect of silver nanoparticles (AgNPs) on the octane number of gasoline was further examined using three-dimensional surface and cube plots, as shown in Figure 6. The interaction between time and concentration at a fixed temperature (35 °C), illustrated in Figure 6a, revealed that increasing both parameters led to a significant improvement in the octane number. This suggests that longer exposure times and higher concentrations of AgNPs enhance catalytic interactions with fuel components. In contrast, Figure 6b, which explores the combined effect of time and temperature at a fixed AgNP concentration (2.06 g L⁻¹), showed a nearly flat surface with minimal variation in octane number. This indicates that at low concentration levels, the influence of time and temperature is limited, likely due to insufficient nanoparticle activity. Figure 6c presents the interaction between temperature and concentration at a fixed time (5.95 h), where a notable increase in octane number is observed with increasing both parameters. This demonstrates a synergistic effect, potentially resulting from enhanced nanoparticle dispersion or reactivity at elevated temperatures. Finally, the cube plot in Figure 6d provides a visual representation of the predicted octane values at the extremes of the design space. The highest values (above 87%) were achieved at high concentration and medium temperature, while the lowest values (around 80%)

corresponded to the lowest levels of all factors. These results confirm that while time and temperature play supporting roles, AgNP concentration is the most influential factor in improving gasoline octane number. The octane number measurements exhibited a very low standard deviation (0.0684) and coefficient of variation (0.0819%), indicating excellent reproducibility and minimal experimental variability. The overall mean octane number across all experimental runs was 83.58 ± 0.0684 (SD), with individual values ranging from 80 to a maximum of 87, depending on the specific reaction conditions.

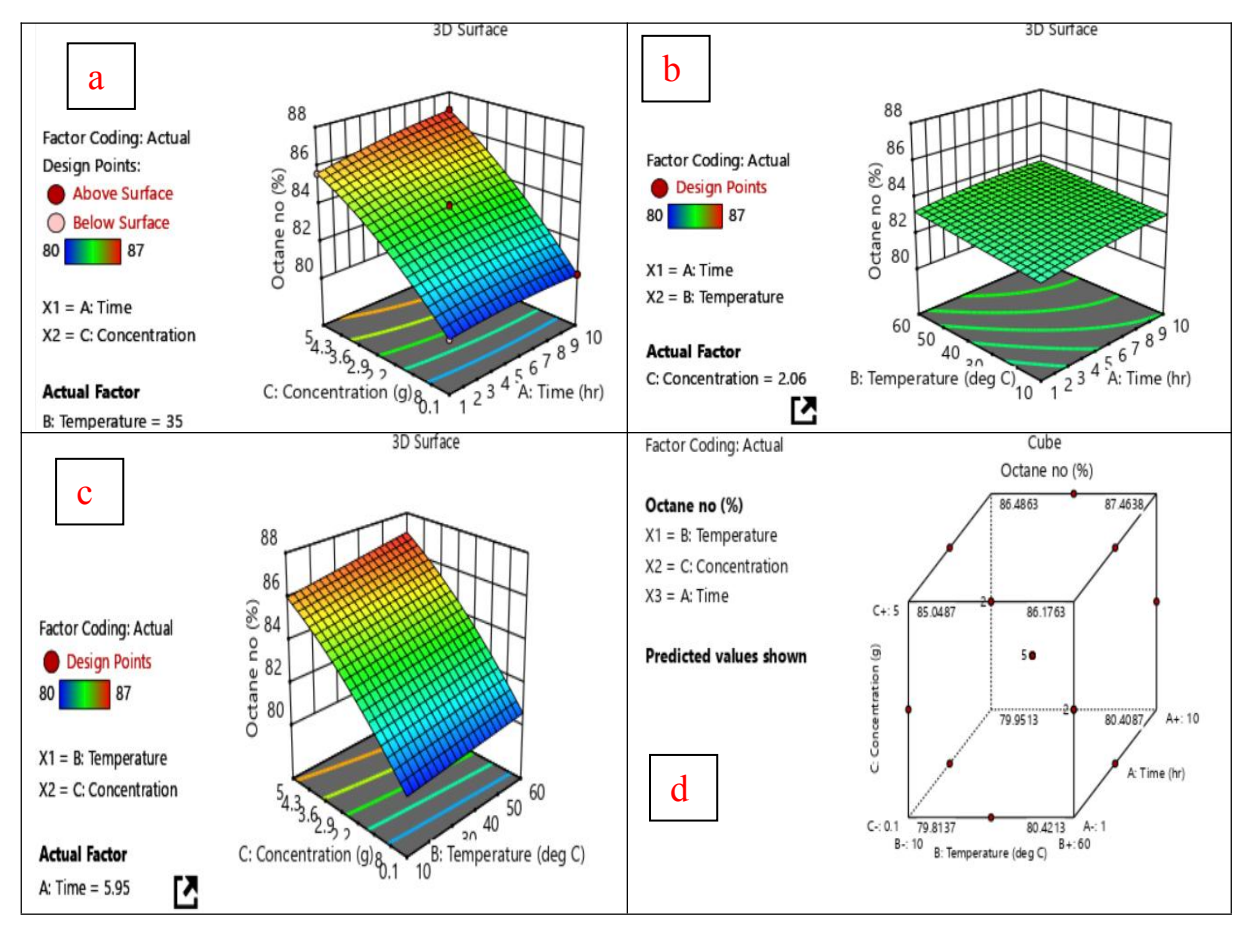


Figure 6: 3D response surface and cube plots showing the effects of silver nanoparticle (AgNP) concentration, temperature, and time on octane number. Subfigures (a-c) illustrate pairwise interactions at constant values of the third factor, while (d) displays predicted octane values across the experimental design space.

3.2.2. Effect on Flash Point

The ANOVA analysis for the quadratic model of the flash point response showed that the model is statistically significant (F-value = 192.59, p < 0.0001), indicating a strong relationship between the experimental variables and the response. Among the tested factors, the concentration of the additive (Factor C) had a highly significant effect on the flash point (F = 1609.54, p < 0.0001), both in its linear and quadratic forms (C and C^2). This demonstrates that concentration is the most influential parameter in determining the flash point. In contrast, the effects of time (A) and temperature (B) were not statistically significant at the 95% confidence level (p = 0.0969 and p = 0.0817, respectively), but they were relatively close to the threshold, suggesting a possible minor influence. The interaction terms (AB, AC, and BC) and the quadratic terms of A and B did not show any significant impact on the response. Furthermore, the lack of fit was found to be not significant (p = 0.1308), which confirms that the model fits the experimental data well, with a low residual error (0.1038). These findings show that quadratic model is suitable in predicting the flash point at conditions of the experiment. Table 4 shows the results of analysis of variance (ANOVA) of the quadratic model used to analyze flash point data, which allows understanding the impact of independent variables or time, temperature, and AgNP concentration on each other. The importance of the model and the role of each of the terms allows determining the degree to which these factors affect flash point behavior.

Source	F-value	p-value	Significance	Interpretation
Model	192.59	< 0.0001	Significant	The overall model is highly. it is significant and fits data well.
A - Time	3.67	0.0969	Not significant (close to threshold)	Time has a minor effect; close to statistical significance.
B - Temperature	4.13	0.0817	Not significant (close to threshold)	Flash point can be affected in some way by temperature.
C - Concentration	1609.54	< 0.0001	Highly significant	Concentration is the most influential factor on the flash point.
AB (Interaction)	0.1079	0.7522	Not significant	No significant interaction between Time and Temperature.
AC (Interaction)	0.0607	0.8125	Not significant	No significant interaction between Time and Concentration.
BC (Interaction)	0.0067	0.9369	Not significant	No significant interaction between Temperature and Concentration.
A² (Quadratic term)	0.3782	0.5580	Not significant	The nonlinear effect of Time is not significant.
B² (Quadratic term)	0.1312	0.7279	Not significant	The nonlinear effect of Temperature is not significant.
C² (Quadratic term)	115.73	< 0.0001	Highly significant	Nonlinear effect of Concentration is highly significant.
Lack of Fit	3.46	0.1308	Not significant	The model adequately fits the data; no significant lack of fit.
Residual Error	-	-	-	Residual error is low, supporting model reliability.

3.2.2.1. Final equation in terms of actual factors

The final regression equation (3) for predicting the flash point (in °C) based on the quadratic model is: $Flash\ Point = -43.2423 + 0.0285\ A + 0.0051\ B + 0.1580\ C + 0.00018\ AB + 0.00136\ AC - 0.000082\ BC - 0.00180\ A^2 - 0.0000344\ B^2 + 0.1064\ C^2$ (3)

The final quadratic regression model developed for flash point prediction demonstrated good agreement with the experimental data. The model includes linear, interaction, and quadratic terms for the three studied factors: time (A), temperature (B), and nanoparticle concentration (C). The regression coefficients show that concentration has the most significant impact on flash point, both in linear (0.1580) and quadratic form (0.1064), which aligns with the ANOVA results. Time and temperature had minor linear effects (0.0285 and 0.0051 respectively), and their quadratic and interaction terms were relatively small, suggesting a limited influence. The model is suitable for capturing both direct and nonlinear effects on flash point behavior under the tested conditions.

The diagnostic plots for the flash point model (Figure 7) provided strong evidence supporting the validity and reliability of the regression analysis. The normal probability plot of residuals (Figure 7a) demonstrated that the residuals closely followed a straight line, indicating approximate normal distribution and confirming that the assumption of normality was met. In the residuals vs. predicted values plot (Figure 7b), the residuals appeared randomly scattered around zero with no visible pattern or funnel shape, supporting the assumption of homoscedasticity and confirming that the variance of residuals was constant across all prediction levels. The Cook's Distance plot (Figure 7c) showed that all values remained below the red threshold line (typically set at 1.0), indicating that no single observation had an undue influence on the regression model. This affirms the stability of the data and the robustness of the model's predictions. Lastly, the Box-Cox plot for power transforms (Figure 7d) suggested that no transformation of the response variable was required, as the optimal lambda (λ) value was close to 1. This confirms that the flash point response data were appropriately modeled using the existing regression form. Collectively, these diagnostics confirm that the quadratic model is statistically sound,

satisfies all necessary assumptions, and is suitable for accurately predicting the flash point of gasoline treated with silver nanoparticles.

Diagnostics Graphs for flash point

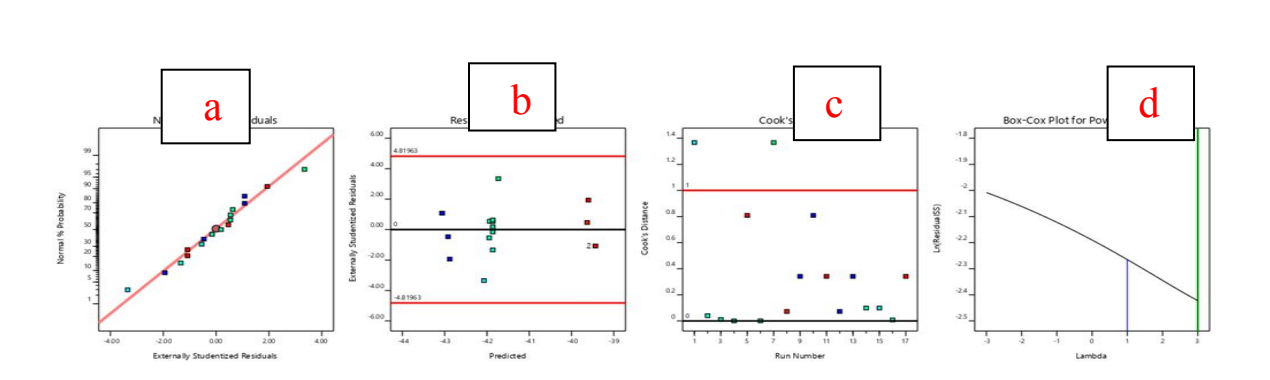
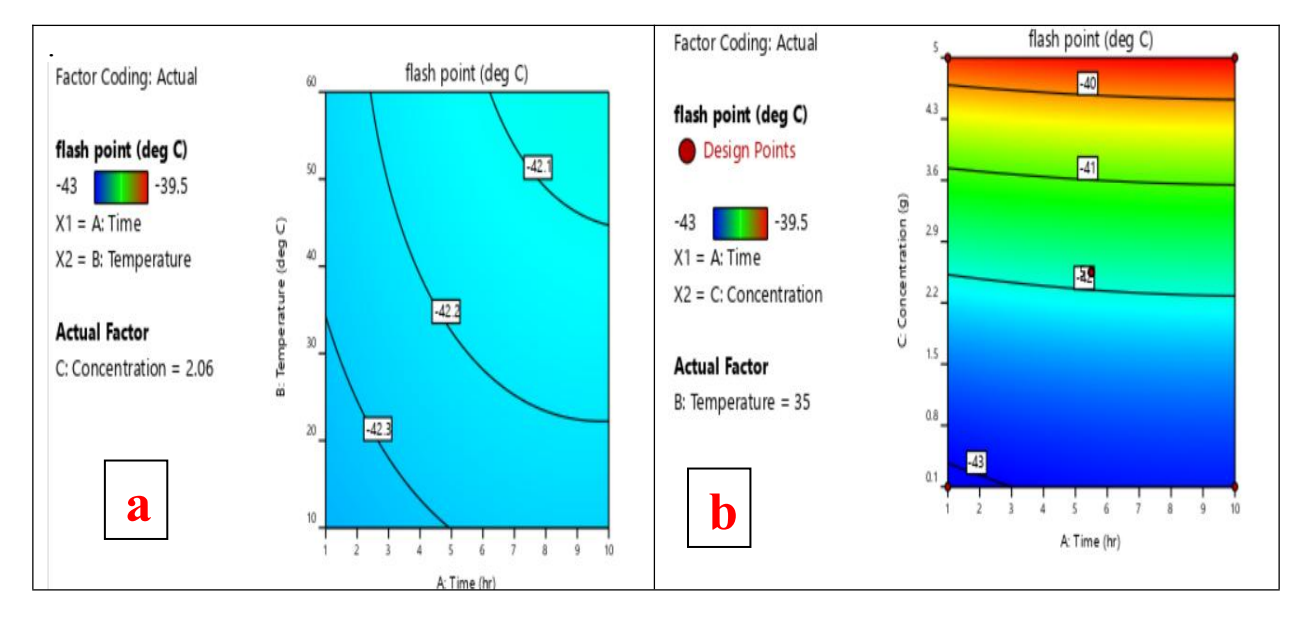


Figure 7: Diagnostic plots for the flash point model showing (a) normal probability plot of residuals, (b) residuals vs. predicted values, (c) Cook's distance for influential points, and (d) Box-Cox plot for response transformation.

The contour plots generated for flash point (Figure 8) offer important visual insights into the interactive effects of process variables such as time, temperature, and silver nanoparticle concentration. In Figure 8a, which plots time against temperature, the flash point appears relatively stable across different durations, with a slight increase observed at lower temperatures and longer reaction times. The nearly horizontal contour lines suggest that both time and temperature have limited combined influence on the flash point. In contrast, Figure 8b—showing time versus concentration—demonstrates a clear and consistent increase in flash point with rising concentration levels, while the effect of time remains minor. The dominant role of concentration is further emphasized by the horizontal alignment of the contour lines. Figure 8c, which maps temperature versus concentration, reveals a steeper vertical gradient, particularly at lower temperatures, indicating that flash point increases significantly with concentration. These graphical trends strongly correlate with the ANOVA findings, which identified concentration as the most statistically significant factor influencing flash point, while temperature and time played relatively lesser roles.



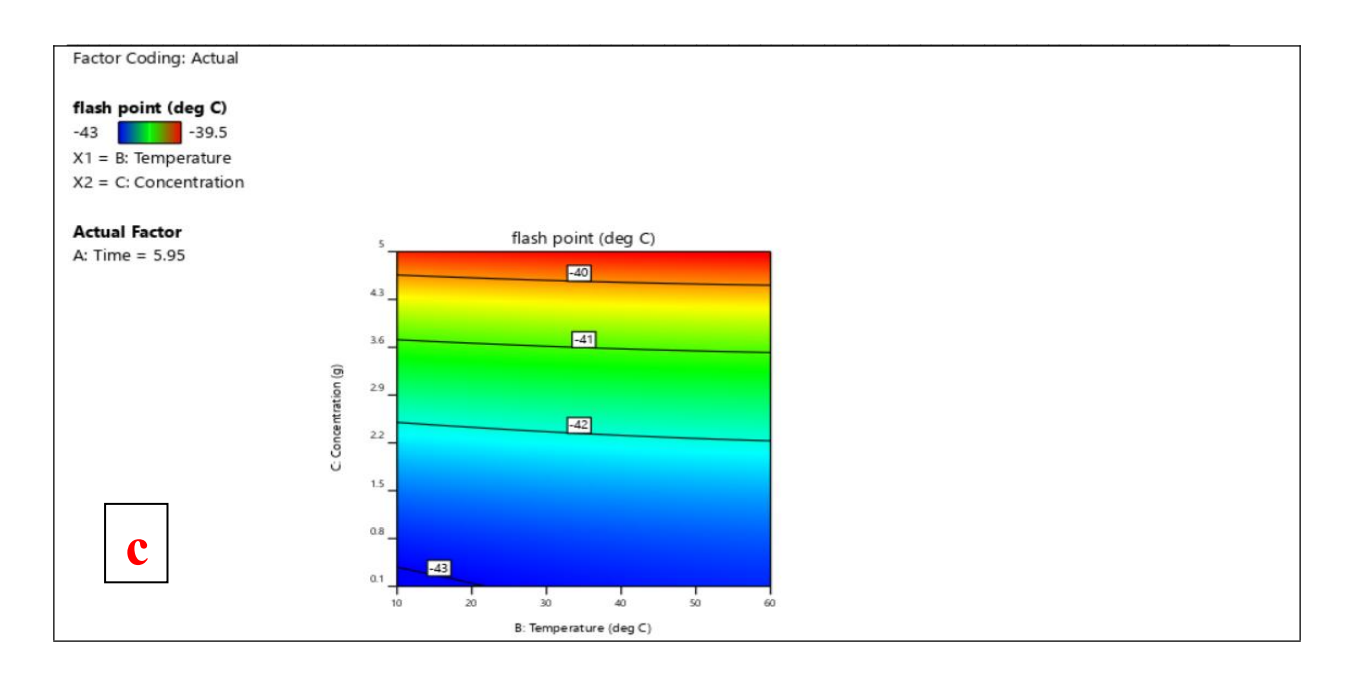


Figure 8: Contour plots showing the interaction effects of (a) time vs. temperature at fixed, (b) time vs. concentration at fixed temperature, and (c) temperature vs. concentration at fixed time on the flash point.

The 3D surface plots presented in Figure 9 provide a clear and comprehensive visualization of how flash point responds to variations in time (A), temperature (B), and nanoparticle concentration (C). The Time vs. Temperature (Figure 9-a) plot displays a nearly flat surface with slight curvature, suggesting weak interaction effects between these two variables. In the Time vs. Concentration (Figure 9-b) surface, flash point increases significantly with rising concentration, while time exerts minimal influence, as reflected by the relatively flat surface along the time axis and a strong gradient along the concentration axis. Similarly, the Temperature vs. Concentration (Figure 9-c) plot indicates that the flash point is primarily affected by concentration; despite changes in temperature, the surface remains nearly parallel along the temperature axis, reaffirming the marginal role of temperature in comparison to concentration. These observations are in full agreement with the ANOVA results, which highlighted concentration as the most significant factor. Furthermore, the 3D cube plot (Figure 9-d) reinforces these findings by offering a spatial perspective of the combined effects of all three variables. Despite lacking color gradients, the cube clearly shows higher flash point values concentrated at the corners with higher nanoparticle concentrations, while variations along the time and temperature axes remain subtle. Overall, both the surface and cube plots confirm that concentration of silver nanoparticles plays a dominant role in enhancing the flash point of gasoline, whereas time and temperature have comparatively minor impacts within the studied experimental range. The flash point measurements exhibited a mean value of - 41.59 °C with a standard deviation of 0.1218 and a coefficient of variation of 0.2928%. Individual flash point values ranged from - 43 °C to -39.5 °C, reflecting the influence of different experimental conditions on volatility.

Several previous studies align with and reinforce our findings, underscoring the broader potential of metal-based nanoparticles as fuel additives. For instance, Fattah et al. (2022) demonstrated that Ag_2O nanoparticles at a mere 0.05 % concentration significantly enhanced combustion efficiency and reduced CO and NO_x emissions by 52 % and 35 %, respectively, in a small gasoline engine[56]. In another recent investigation, metal oxide nanoparticles (including TiO_2 and Ag_2O_3) were found to improve biodiesel performance, reducing fuel consumption by 4.4 % and CO emissions by 16.4% [57]. These findings confirm that even low concentrations of silver-based nanomaterials can exert a strong catalytic influence in hydrocarbon-based fuels. Additionally, a 2023 study on Al_2O_3 and TiO_2 in gasoline reported measurable changes in physicochemical properties such as refractive index and density, illustrating the nuanced impact of nano-additives on fuel characteristics[58, 59]. Together with our data, showing octane number improvement from 80 % to 87% (mean: 83.58 \pm 0.0684 (SD)) and flash point elevation from - 43 °C to -39.5 °C (mean: -41.59 °C \pm 0.2928 (SD)) these results indicate a growing and

consistent body of evidence supporting the efficacy of nanoparticle dopants in enhancing fuel performance, stability, and emissions profile.

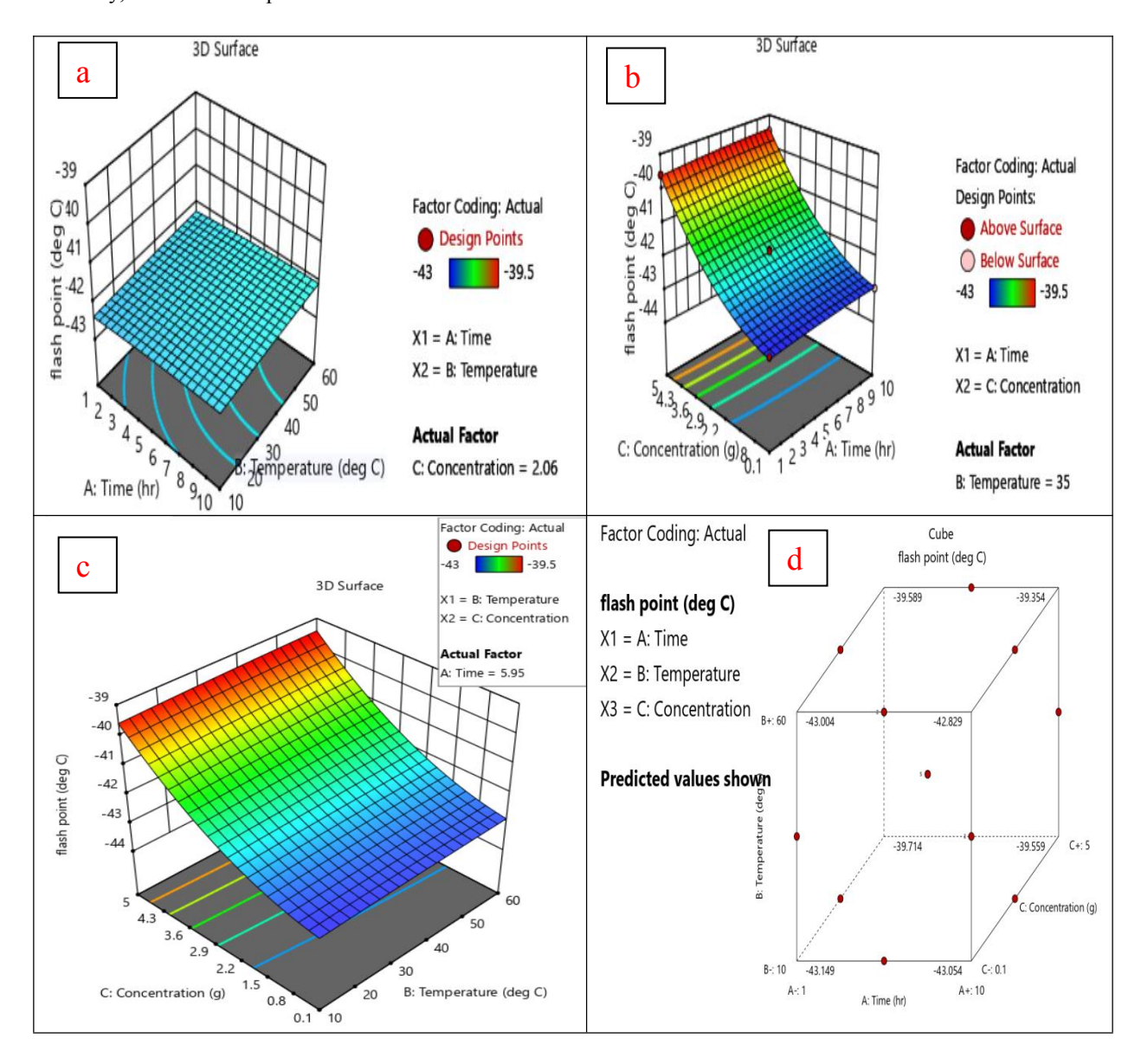


Figure 9: 3D surface plots illustrating the effect of interaction between: (a) time vs. temperature at fixed, (b) time vs. concentration at fixed temperature, and (c) temperature vs. concentration at fixed time on the flash point. (d) displays predicted flash point values across the experimental design space.

3.3. Molecular-level Mechanisms of AgNPs on Combustion and Volatility.

Silver nanoparticles (AgNPs) play a significant role in enhancing combustion chemistry and fuel volatility at the molecular level due to their unique catalytic and thermal properties. Acting as efficient heterogeneous catalysts, AgNPs promote the generation of highly reactive radicals (such as O• and OH•) that accelerate the chain-branching oxidation reactions of hydrocarbon molecules. This results in a faster and more complete combustion process, thereby improving fuel energy release and reducing knocking tendencies, which directly contributes to increasing the octane number .The large surface-to-volume ratio of AgNPs allows for better interaction and adsorption of fuel molecules, improving micro-mixing and promoting more uniform vaporization. This enhanced volatility helps in achieving smoother and more stable flame propagation, ultimately contributing to more efficient combustion and affecting the flash point by facilitating easier ignition.

In this study, the concentration of AgNPs was found to be the dominant factor influencing combustion performance, while variations in mixing time and pre-combustion temperature showed minimal effects. This is because concentration directly determines the number of active catalytic sites available to initiate and sustain the combustion-enhancing reactions. Higher concentrations provide more catalytic surfaces, significantly boosting radical generation and heat transfer effects.

On the other hand, the time and temperature used during mixing primarily aid in achieving better dispersion and homogeneity of nanoparticles within the fuel but do not initiate chemical activation or significantly alter molecular-level interactions before combustion. The actual catalytic activity of AgNPs is only fully realized under the high-temperature environment of combustion (often exceeding 1500 °C), where rapid reaction kinetics dominate. Thus, once nanoparticles are well dispersed, extending mixing time or increasing pre-mixing temperature does not markedly influence fuel properties. Overall, these findings suggest that optimizing AgNP concentration is a more effective and practical strategy for improving fuel properties such as octane number and flash point than altering mixing parameters.

3.4. Limitations and Implications

While the incorporation of silver nanoparticles (AgNPs) demonstrated significant improvements in gasoline properties, particularly in enhancing octane number and flash point, certain limitations must be acknowledged. The data revealed that nanoparticle concentration was the most influential factor in both responses. For instance, increasing AgNPs concentration from 0.1 g to 5 g resulted in a rise in octane number from 80% to 87%, and a corresponding increase in flash point from - 43°C to - 39.5°C, indicating a clear positive correlation. However, the effects of reaction time and temperature were consistently minimal, as confirmed by low F-values and high pvalues in the ANOVA tables (p > 0.05 for time and temperature in both octane number and flash point models). This narrow response range suggests that outside of concentration, the experimental design had limited sensitivity to other variables. Additionally, while the quadratic model used in the regression analysis achieved a high degree of fit ($R^2 = 0.986$ for octane number and $R^2 = 0.963$ for flash point), residual diagnostic plots revealed slight deviations from normality and a few influential points (Cook's distance > 1), indicating potential areas for refinement in model accuracy. These limitations imply that future studies should expand the experimental space or explore synergistic effects with other nanomaterials to fully capture the interactive behavior of process parameters. Nonetheless, the findings offer strong practical implications: optimizing nanoparticle concentration can lead to measurable improvements in fuel performance, making silver-based nanofuels a promising and scalable avenue for cleaner and more efficient combustion systems. It is important to consider the economic aspects of using silver nitrate (AgNO₃) in catalyst preparation. Despite its proven effectiveness in improving gasoline combustion, AgNO₃ is relatively expensive, and increasing its concentration directly affects the overall production cost. Future studies should focus on optimizing the silver content or exploring alternative, less costly metal precursors to achieve a balance between performance enhancement and economic feasibility.

This study demonstrates the significant potential of silver-based nanoparticles (Ag and AgCl) in enhancing fuel performance. However, it is essential to consider potential engine-compatibility issues associated with their use. One primary concern is the possible formation of deposits or residues resulting from incomplete combustion or nanoparticle agglomeration. These deposits could lead to injector clogging, increased particulate matter, or changes in spray characteristics, ultimately affecting combustion efficiency and long-term engine durability. Silver-based compounds may pose a risk of corrosion, especially when exposed to high-temperature environments and acidic by-products within the combustion chamber. Although silver exhibits relatively high thermal stability and corrosion resistance under standard conditions, the presence of chlorides (as in AgCl) may exacerbate corrosion in metal components due to the potential formation of silver chloride residues that can be reactive under certain conditions. To mitigate these risks, it is recommended that further long-term engine tests be conducted to assess deposit formation, material compatibility, and any potential effects on exhaust after-treatment systems. Additionally, optimizing nanoparticle concentration and ensuring proper dispersion within the fuel matrix can help minimize agglomeration and residue-related issues. These considerations are crucial to ensure that the observed fuel performance improvements translate into practical, safe, and sustainable engine applications.

Regarding scalability and cost-effectiveness, biogenic (green-synthesized) silver nanoparticles (AgNPs) offer both opportunities and challenges for industrial fuel additive applications. On one hand, biosynthesis methods are

considered environmentally friendly and can serve as potentially lower-cost alternatives to traditional chemical or physical nanoparticle synthesis. Examples include the use of plant extracts, bacteria, or fungi. These methods eliminate the need for harsh chemicals and high-energy inputs, contributing to safer and more sustainable large-scale production.

However, achieving consistent quality and uniform particle size distribution at an industrial scale remains a significant challenge. Batch-to-batch variability, long reaction times, and difficulties in controlling shape and aggregation can increase overall production costs and affect reproducibility. Moreover, the cost of raw silver and the requirement for downstream purification (e.g., removing residual biomolecules) can further impact economic feasibility. Despite these hurdles, ongoing advancements in green nanotechnology and bioprocess optimization continue to improve yield and scalability. If properly optimized, biogenic AgNP production could become a cost-effective and eco-friendly approach, making it suitable for large-scale fuel additive applications while aligning with stricter environmental regulations. Nonetheless, comprehensive techno-economic assessments and pilot-scale studies are still needed to fully establish commercial viability.

4. Conclusion

gasoline enhancement, particularly in improving octane number and flash point—two critical indicators of fuel efficiency and safety. The experimental results clearly show that increasing AgNP concentration leads to a marked improvement in fuel quality, with the octane number rising from 80% to 87%, and the flash point improving from -43°C to -39.5 °C. Statistical and surface response analyses confirmed that nanoparticle concentration is the dominant factor influencing these outcomes, while time and temperature showed only weak effects within the studied range. Importantly, the superior performance of the AgNPs may be attributed not only to their inherent catalytic properties but also to their biogenic synthesis using Jatropha seed extract, which may impart unique surface characteristics, improved dispersion, and enhanced interaction with hydrocarbon molecules. The use of Jatropha-based green synthesis is not only environmentally sustainable but also aligns with the broader push toward bio-integrated fuel technologies. Furthermore, silver nanoparticles have shown synergistic potential in previous studies related to biodiesel enhancement, where they promoted better atomization, improved thermal stability, and reduced ignition delay. This suggests that the same biogenically synthesized AgNPs evaluated in this study could have dual functionality—benefiting both petroleum-based fuels like gasoline and biofuels such as biodiesel. These findings pave the way for future integrated fuel formulations that combine the performance of nanotechnology with the sustainability of bio-based additives. In conclusion, silver nanoparticles especially those synthesized from Jatropha represent a promising frontier in the development of advanced, highperformance, and cleaner-burning fuels. Further studies are encouraged to explore their role in full-scale engine testing, emissions analysis, and hybrid fuel systems.

5. Recommendations for Future Work

Based on the promising outcomes of this study, several directions are recommended for future research. Firstly, extended engine performance and emission testing should be conducted to evaluate the real-world impact of AgNP-doped gasoline under dynamic combustion conditions. Such investigations will help confirm the fuel economy benefits and quantify reductions in harmful emissions such as CO, NO_x, and unburned hydrocarbons. Secondly, it is advisable to explore long-term fuel stability and nanoparticle dispersion behavior in storage environments, as agglomeration may alter efficacy over time. Incorporating surface modifiers or bio-compatible stabilizers could help maintain consistent performance.

Thirdly, further comparative studies using AgNPs synthesized from different plant sources or using chemical vs. green synthesis routes would shed light on the influence of particle origin, morphology, and surface chemistry on fuel properties. This could also include examining size-dependent effects and surface -area-to-volume ratios to optimize nanoparticle performance.

Moreover, extending the application of Jatropha-based AgNPs to biodiesel systems or blended fuels (e.g., gasoline-biodiesel mixtures) would offer a valuable perspective on their multifunctionality and eco-compatibility. Investigating their compatibility with alternative fuels supports the broader goal of achieving sustainable and integrated nanofuel technologies.

Lastly, a techno-economic analysis should be performed to assess the scalability and commercial viability of producing biogenic silver nanoparticles for industrial fuel enhancement. This would involve life cycle assessment, cost-benefit analysis, and evaluation of environmental trade-offs.

Conflict of interest:

There is no conflict of interest.

References:

- 1. Hatami, M., *Nanomaterials in fuel additives, lubricants, and engine oils*, in *Handbook of Nanomaterials, Volume 1.* 2024, Elsevier. p. 593-616. DOI: 10.1016/b978-0-323-95511-9.00029-9.
- 2. Abdul Jameel, A.G., et al., *Predicting Octane Number Using Nuclear Magnetic Resonance Spectroscopy and Artificial Neural Networks.* Energy & Fuels, 2018. **32**(5): p. 6309-6329. DOI: 10.1021/acs.energyfuels.8b00556.
- 3. Alboqami, F., et al., *A Methodology for Designing Octane Number of Fuels Using Genetic Algorithms and Artificial Neural Networks.* Energy & Fuels, 2022. **36**(7): p. 3867-3880. DOI: 10.1021/acs.energyfuels.1c04052.
- 4. Khoirudin, et al., *Flash Point Improvement of Mineral Oil Utilizing Nanoparticles to Reduce Fire Risk in Power Transformers: A Review.* Fire 2024. 7(9): p. 305. DOI: 10.3390/fire7090305
- 5. Tipler, S., et al., *Predicting octane numbers relying on principal component analysis and artificial neural network.* Computers & Chemical Engineering, 2022. **161**: p. 107784. DOI: 10.1016/j.compchemeng.2022.107784.
- 6. Shah, V., et al., *A comprehensive study on applications of nanomaterials in petroleum upstream and downstream industry.* Environmental Science and Pollution Research, 2024. **31**(10): p. 14406-14423. DOI: 10.1007/s11356-023-31569-3.
- 7. Sarlak, M., et al., *Combustion of gasoline with oxygen-containing and nano-additives: An experimental study, modeling, optimization, and analysis survey.* Journal of the Taiwan Institute of Chemical Engineers, 2024. **159**: p. 105452. DOI: 10.1016/j.jtice.2024.105452.
- 8. Ferdous, A.R., et al., *Advancements in nanotechnology applications: Transforming catalysts, sensors, and coatings in petrochemical industries.* Fuel, 2024. **371**: p. 132020. DOI: 10.1016/j.fuel.2024.132020.
- 9. Alhajj, M., et al., *Enhanced fluorescence response and effective petroleum sensing performance of silver/copper nanocomposites.* Materials Chemistry and Physics, 2025. **333**: p. 130342. DOI: 10.1016/j.matchemphys.2024.130342.
- 10. Barghout, M.E. and A. Samy, *The Acaricidal Impact of Green Synthesized Zinc Oxide Nanoparticles Against Caloglyphus mycophagous and Mycetoglyphus fungivorus (Family:Acaridae) %J Egyptian Journal of Chemistry.* 2023. **66**(13): p. 1125-1131. DOI: 10.21608/ejchem.2023.204991.7839.
- 11. El Sayed, H.A., et al., *Deep catalytic desulphurization of heavy gas oil at mild operating conditions using self-functionalized nanoparticles as a novel catalyst.* Industrial & Engineering Chemistry Research, 2017. **209**(16): p. 127-131. DOI: 10.1021/acs.iecr.9b06058.
- 12. Khayal, A., et al., *Recent Advances in the Applications of Nanotechnology and Nanomaterials in the Petroleum Industry: A Descriptive Review.* Particle & Particle Systems Characterization, 2023. **40**(8): p. 2300029. DOI: 10.1002/ppsc.202300029.
- 13. Yakın, A. and R. Behçet, *Effect of different types of fuels tested in a gasoline engine on engine performance and emissions.* International Journal of Hydrogen Energy, 2021. **46**(66): p. 33325-33338. DOI: 10.1016/j.ijhydene.2021.07.133.
- 14. Badra, J., et al., *Understanding of the octane response of gasoline/MTBE blends.* Fuel, 2022. **318**: p. 123647. DOI: 10.1016/j.fuel.2022.123647.
- 15. Elkelawy, M., et al., *Impact of Gasoline Fuel Commercial Additive Properties on Engine Performance and Emissions Characteristics*. Pharos Engineering Science Journal, 2025. **2**(1): p. 87-105. DOI: 10.21608/pesj.2025.354037.1014.
- 16. Abdellatief, T.M.M., et al., *Uniqueness technique for introducing high octane environmental gasoline using renewable oxygenates and its formulation on Fuzzy modeling*. Sci Total Environ, 2022. **802**: p. 149863. DOI: 10.1016/j.scitotenv.2021.149863.
- 17. Abdellatief, T.M.M., et al., Recent trends for introducing promising fuel components to enhance the anti-knock quality of gasoline: A systematic review. Fuel, 2021. 291: p. 120112. DOI: 10.1016/j.fuel.2020.120112.
- 18. Borah, D., H. Nath, and H.J.R.i.I.C. Saikia, *Modification of bentonite clay & its applications: A review.* De Gruyter Brill, 2022. **42**(3): p. 265-282.
- 19. Jarullah, A.T., et al., *Production of Green Fuel Using a New Synthetic Magnetite Mesoporous Nano-Silica Composite Catalyst for Oxidative Desulfurization: Experiments and Process Modeling.* 2024. **14**(8): p. 529. DOI: 10.3390/catal14080529

- 20. Chauhan, P., et al., *Nano-bioremediation: an eco-friendly and effective step towards petroleum hydrocarbon removal from environment.* Environ Res, 2023. **231**(Pt 2): p. 116224. DOI: 10.1016/j.envres.2023.116224.
- 21. Kumari, S., A. Srivastava, and S. Sengupta, *Development of silver dichromate-geopolymer composite: An innovative catalyst for simultaneous desulfurization and denitrogenation for cleaner petroleum fuel.* Separation and Purification Technology, 2025. **358**: p. 130369. DOI: 10.1016/j.seppur.2024.130369.
- 22. Mohsen, A. and M.A. Abdel-Goad, *Silver Nanoparticles from Nature: Green Synthesis Methods and Applications A Review.* Journal of Advanced Engineering Trends, 2025. **44**(1): p. 227-236. DOI: 10.21608/jaet.2024.319157.1334.
- 23. Abdullah, M.M.S. and H.A. Al-Lohedan, *Nanomaterials in petroleum industry*, in *Handbook of Nanomaterials, Volume 1.* 2024, Elsevier. p. 617-648. DOI: 10.1016/b978-0-323-95511-9.00003-2.
- 24. Li, G., et al., *Review on advances in adsorption material for mercaptan removal from gasoline oil.* Journal of Industrial and Engineering Chemistry, 2024. **139**: p. 36-55. DOI: 10.1016/j.jiec.2024.05.008.
- 25. Pourhosseinhendabad, P. and P. Z Firouzabadi, *From raw to nano: optimized purification and nano-bentonite synthesis for advanced applications.* Physica Scripta, 2025. **100**(6): p. 065916. DOI: 10.1088/1402-4896/add2a9.
- 26. Senniangiri, N., et al., *Effect of SnO2 and Ag nano-additives on the performance, combustion and emission characteristics of diesel engine fueled with mango seed biodiesel.* Petroleum Science and Technology, 2022. **42**(4): p. 470-490. DOI: 10.1080/10916466.2022.2120501.
- 27. El Naggar, A.M.A., et al., *New Approach for Catalytic Production of Ultralow-Sulfur Diesel Fuels Using Binary Composed Catalysts Consisting of Cobalt Nanoparticles.* Industrial & Engineering Chemistry Research, 2020. **59**(16): p. 7277-7290. DOI: 10.1021/acs.iecr.9b06058.
- 28. Metwally, U., et al., *Poly N-(2-aminoethyl) acrylamide-NiO composite as novel efficient photocatalyst for desulfurization of diesel fuel under visible-light irradiation.* Egyptian Journal of Chemistry, 2021. **64**: p. 6029-6041. DOI: 10.21608/ejchem.2021.74733.3681.
- 29. El Naggar, A.M.A., et al., *Synthesis of acrylamide-copper oxide hybrid structure as a novel photocatalyst for visible-light induced desulphurisation of petroleum diesel fuel.* International Journal of Environmental Analytical Chemistry, 2023. **104**(20): p. 9164-9185. DOI: 10.1080/03067319.2023.2226072.
- 30. Gómez-Gómez, A.L., et al., *Green synthesis of gold nanoparticles by curcin from Jatropha curcas: Characterization and antibacterial activity.* 2024. **9**(5): p. 254-258.
- 31. Saifuddin, N.N., et al., *Potentials of roots, stems, leaves, flowers, fruits, and seeds extract for the synthesis of silver nanoparticles.* Bioprocess Biosyst Eng, 2024. **47**(8): p. 1119-1137. DOI: 10.1007/s00449-024-03044-x.
- 32. Habeeba, U. and N. Raghavendra, *Green synthesis and antioxidant potency of silver nanoparticles using arecanut seed extract.* Nano-Structures & Nano-Objects, 2024. **38**: p. 101118. DOI: 10.1016/j.nanoso.2024.101118.
- 33. Siswanto, E.E. Yunata, and I.K. Firdaus. *The effect of temperature and reductant concentration on the biosynthesis of silver nanoparticles (Ag-NPs) from Jatropha leaf extract (Jatropha curcas L.).* in *AIP Conference Proceedings.* 2024. AIP Publishing LLC. DOI: 10.1063/5.0195727.
- 34. Basosila, N.B., et al., *Efficacy of silver nanoparticles from Jatropha curcas leaf extracts against pyrethroid-resistant Anopheles gambiae.* orapuh, 2024. **5**(5): p. e1147-e1147. DOI: 10.4314/orapj.v5i5.47.
- 35. Nag, S., et al., *Biosynthesis of Nanoparticles from Jatropha curcas Latex*, in *Nanomaterials in Agroforestry Systems*. 2025, Springer. p. 99-125. DOI: 10.1007/978-981-96-1337-3 5.
- 36. Golthi, V. and J.J.I. Kommu, *Bio-Fabrication of Silver Nanoparticles Using Jatropha podagrica leaf extract: Photodegradation of dyes and antibacterial properties.* 2024. **30**(11): p. 7699-7710. DOI: 10.1007/s11581-024-05829-2.
- 37. Heikal, M., et al., Effect of Jatropha Seed Extract–Mediated Green Synthesis of Silver Nanoparticle on Staphylococcus aureus Isolated from Clinical Mastitis. Egyptian Journal of Veterinary Sciences, 2025: p. 1-12. DOI: 10.21608/ejvs.2024.332160.2457.
- 38. Hoth, A. and C.P. Kolodziej, *Effects of knock intensity measurement technique and fuel chemical composition on the research octane number (RON) of FACE gasolines: Part 1 Lambda and knock characterization.* Fuel, 2021. **304**: p. 120722. DOI: 10.1016/j.fuel.2021.120722.
- 39. Lopez-Pintor, D., J. Dec, and S. Cho, *Performance of octane index in LTGC engines from beyond MON to beyond RON.* Fuel, 2023. **341**: p. 127625. DOI: 10.1016/j.fuel.2023.127625.
- 40. Lyu, D., et al., *Octane Response of Gasoline Fuels to Different Antiknock Oxygenates Addition.* Journal of Energy Resources Technology, Part A: Sustainable and Renewable Energy, 2025. **1**(3). DOI: 10.1115/1.4067060.

- 41. Kovaleva, E.B., et al., *A New Approach to Determining the Blending Octane Number of Gaseous Components of Motor Gasolines.* Inorganic Materials, 2024. **60**(1): p. 45-51. DOI: 10.1134/s0020168524700079.
- 42. Hoth, A., *Investigation of Operational Parameter Differences Between the Standard RON Test Method and Knock-Limited Modern Spark-Ignition Engine Operation*. 2024, Michigan Technological University. DOI: 3054745108/se-2.
- 43. Robeyn, T., et al., *A Pressure-Oscillation-Based RON Estimation Method for Spark Ignition Fuels beyond RON 100.* energies, 2024. **17**(6): p. 1362. DOI: 10.3390/en17061362
- 44. Abdellatief, T.M.M., et al., *Novel variants conceptional technology to produce eco-friendly sustainable high octane-gasoline biofuel based on renewable gasoline component.* Fuel, 2024. **366**: p. 131400. DOI: 10.1016/j.fuel.2024.131400.
- 45. Aljaman, B., et al., A comprehensive neural network model for predicting flash point of oxygenated fuels using a functional group approach. Fuel, 2022. 317: p. 123428. DOI: 10.1016/j.fuel.2022.123428.
- 46. Tugyi, L., Z. Siménfalvi, and G.L. Szepesi, *Determination of Flash Points of Flammable Mixtures for Explosion Protection.* Solid State Phenomena, 2024. **363**: p. 81-86. DOI: 10.4028/p-tky3Si.
- 47. Firman, M., et al. *Characterization of used oil distillate at various distillation temperatures as diesel fuel.* in *IOP Conference Series: Earth and Environmental Science.* 2021. IOP Publishing. DOI: 10.1088/1755-1315/758/1/012020.
- 48. Idris, S.A.M. and G.G.A. Jalgaf, *Optimizing Kerosene Blends with Heavy Naphtha and Diesel to Achieve Aviation Fuel Standards: A Study of Flash Point, Specific Gravity, and Boiling Point Characteristics.* SSRN. DOI: 10.2139/ssrn.5099650.
- 49. Deering, C.E., et al., *The flash point of elemental sulfur: Effect of heating rates, hydrogen sulfide, and hydrocarbons.* Results in Engineering, 2022. **16**: p. 100629. DOI: 10.1016/j.rineng.2022.100629.
- 50. Varaprasad, K., et al., *Development, Characterization, and Biomedical Applications of PVP–AgCl Nanomaterials: Antibacterial and Anticancer Properties.* ChemistrySelect, 2024. **10**(1): p. e202404398. DOI: 10.1002/slct.202404398.
- 51. Yin, L., et al., *Lignosulfonate as a versatile regulator for the mediated synthesis of Ag@AgCl nanocubes.* Nanoscale, 2025. **17**(5): p. 2451-2461. DOI: 10.1039/d4nr04161e.
- 52. Ng, A.K., H. Koh, and E. Detsi, *Tri-layer nanoporous silver | gold | silver by etching without sacrificing materials through the Kirkendall effect.* Acta Materialia, 2025. **284**: p. 120574. DOI: 10.1016/j.actamat.2024.120574.
- 53. Dingyi, L., et al., *In Situ SERS Monitoring the Visible Light Photocatalytic Degradation of Nile Blue on Ag@AgCl Single Hollow Cube as a Microreactor.* ChemistrySelect, 2018. **3**: p. 428-435. DOI: 10.1002/slct.201702545.
- 54. Alam, M.A., et al., *X-ray crystallographic diffraction study by whole powder pattern fitting (WPPF) method: Refinement of crystalline nanostructure polymorphs TiO2.* South African Journal of Chemical Engineering, 2025. **51**: p. 68-77. DOI: 10.1016/j.sajce.2024.10.010.
- 55. Nadjia, L. and E. Abdelkader, *Design, synthesis and characterization of ceria: assessment of crystallite size and intrinsic strain using XRD profile analysis and its photocatalytic applications.* Journal of the Iranian Chemical Society, 2024. **22**(2): p. 297-324. DOI: 10.1007/s13738-024-03149-w.
- 56. Fattah, A.A., et al., *Utilization of Selected Nanoparticles (Ag2O and MnO2) for the Production of High-Quality and Environmental-Friendly Gasoline.* Sustainability, 2022. **14**(19): p. 12513. DOI: 10.3390/su141912513.
- 57. Ghadhban, S.A., H. Al-Gburi, and I.W. Maid, *Exploring Experimentally Al2O3 Nanoparticles Impact on a Four-Stroke Diesel Engine's Performance and Emissions*. International Journal of Heat and Technology, 2024. **42**(6): p. 1994-2000. DOI: 10.18280/ijht.420616.
- 58. Mohan, S., A.B.V. Barboza, and P. Dinesha, *Effect of eco-friendly nano additive with green fuel on performance and emissions of a compression ignition engine.* Cogent Engineering, 2023. **10**(2): p. 2272351. DOI: 10.1080/23311916.2023.2272351.
- 59. Yusof, S.N.A., et al., *A comprehensive review of the influences of nanoparticles as a fuel additive in an internal combustion engine (ICE).* Nanotechnology Reviews, 2020. **9**(1): p. 1326-1349. DOI: 10.1515/ntrev-2020-0104.